

$\eta$ ,  $\omega$  AND CHARMED MESIC NUCLEI <sup>1</sup>

K. Tsushima

*Special Research Center for the Subatomic Structure of Matter (CSSM)  
and Department of Physics and Mathematical Physics  
The University of Adelaide, SA 5005, Australia  
E-mail: ktsushim@physics.adelaide.edu.au*

**Abstract**

Using the quark-meson coupling (QMC) model, we investigate theoretically whether  $\eta$  and  $\omega$  mesons form meson-nucleus bound states. We study several nuclei from  ${}^6\text{He}$  to  ${}^{208}\text{Pb}$ , including those which are the final nuclei in the proposed experiment at GSI. Results for the  $\omega$  are compared with those of the Walecka model. Our results suggest that one should expect to find  $\eta$ - and  $\omega$ -nucleus bound states in all these nuclei. Furthermore, we investigate the possibility of charmed mesic nuclei. It is shown that the  $D^-$  meson will inevitably form narrow bound states with  ${}^{208}\text{Pb}$ .

**Key-words:** Meson-nucleus bound states, Quark-meson coupling model, Nuclear medium, In-medium meson mass, Chiral symmetry in medium

## 1 Introduction

The study of the properties of hadrons in a dense and/or hot nuclear medium is one of the most exciting new directions in nuclear physics. In particular, the medium modification of the light vector ( $\rho$ ,  $\omega$  and  $\phi$ ) meson masses is expected to provide us information concerning chiral symmetry (restoration) in a nuclear medium.

For example, the experimental data obtained at the CERN/SPS by the CERES [2] and HELIOS [3] collaborations has been interpreted as evidence for a downward shift of the  $\rho$  meson mass in dense nuclear matter [4]. Further experiments are planned at TJNAF [5] and GSI [6] to measure the dilepton spectrum from vector mesons produced in nuclei.

Recently, a new, alternative approach to study meson mass shifts in nuclei was suggested by Hayano *et al.* [7], involving the (d,  ${}^3\text{He}$ ) reaction to produce  $\eta$  and  $\omega$  mesons with nearly zero recoil. If the meson feels a large enough, attractive (Lorentz scalar) force inside a nucleus, the meson is expected to be bound. This may be regarded as a consequence of the partial restoration of chiral symmetry.

Stimulated by this experimental proposal, theoretical investigations have been made by Hayano *et al.* [8], Klingl *et al.* [9] and our group [10] for various  $\eta$ - and  $\omega$ -mesic nuclei, including those which are the final nuclei in the proposed experiment. Our investigations on the mesic nuclei have been based on the quark-meson coupling (QMC) model (and the

<sup>1</sup> Invited talk at the XIV International Seminar on High Energy Physics Problems "Relativistic Nuclear Physics and Quantum Chromodynamics", Dubna, Aug. 17-22, 1998

Walecka model for the  $\omega$ ). A detailed description of the QMC model which is relevant for this report can be found in Refs. [11] - [16].

The result for the  $\omega$ -meson is especially interesting. Because it consists of almost pure light quark-antiquark pairs,  $q\bar{q}$  ( $q = u, d$ ), in an isoscalar nucleus the  $q$  and  $\bar{q}$  feel equal and opposite vector potentials. This means that the effect of the Lorentz scalar potential is unmasked which leads to expectations of quite deeply bound  $\omega$ -nucleus states [7] - [10].

Concerning charmed mesic nuclei, it is in some ways even more exciting, in that it promises more specific information on the relativistic mean fields in nuclei and the nature of dynamical chiral symmetry breaking. We focus on systems containing an anti-charm quark and a light quark,  $\bar{c}q$ , which have no strong decay channels if bound. If we assume that dynamical chiral symmetry breaking is the same for the light quark in the charmed meson as in purely light-quark systems, we expect the same coupling constant,  $g_c^q$ , in the QMC model.

In the absence of any strong interaction, the  $D^-$  will form atomic states, bound by the Coulomb potential. The QMC model is used here to estimate the effect of the strong interaction. The resulting binding for, say, the 1s level in  $^{208}\text{Pb}$  is between ten and thirty MeV and should provide a very clear experimental signature. On the other hand, although we expect the  $D$ -meson (systems of  $\bar{q}c$ ) will form deeply bound  $D$ -nucleus states, they will also couple strongly to open channels such as  $DN \rightarrow B_c(\pi's)$ , with  $B_c$  a charmed baryon. Thus, it requires an accurate calculation for the widths in a nucleus to estimate the bound state energies relevant for the experimental measurements. Unfortunately, because our present knowledge does not permit such an accurate calculation of the corresponding widths, results for the  $D$ -mesic nuclei may not give useful information for experimenters.

## 2 Meson masses in nuclear matter and finite nuclei

First, we show in Fig. 1 the mass shifts of the  $\eta, \omega$  and  $D(\bar{D})$  mesons, calculated in symmetric nuclear matter [10, 17]. The masses for the  $\eta$  and  $\omega$  are calculated using the physical states, i.e., the superpositions of the octet and singlet states with the mixing angles,  $\theta_P$  for the  $\eta - \eta'$  and  $\theta_V$  for the  $\phi - \omega$  [18]:

$$\xi = \xi_8 \cos \theta_{P,V} - \xi_1 \sin \theta_{P,V}, \quad \xi' = \xi_8 \sin \theta_{P,V} + \xi_1 \cos \theta_{P,V}, \quad (1)$$

with

$$\xi_1 = \frac{1}{\sqrt{3}} (u\bar{u} + d\bar{d} + s\bar{s}), \quad \xi_8 = \frac{1}{\sqrt{6}} (u\bar{u} + d\bar{d} - 2s\bar{s}), \quad (2)$$

$$(\xi, \xi') = (\eta, \eta') \quad \text{or} \quad (\phi, \omega), \quad (3)$$

where the values,  $\theta_P = -10^\circ$  and  $\theta_V = 39^\circ$  [18] are used.

One can easily see that the effect of the singlet-octet mixing is negligible for the  $\omega$  mass in matter, whereas it is important for the  $\eta$  mass. In addition,  $(m_{D,\bar{D}} - m_{D,\bar{D}}^*) \simeq \frac{1}{3}(m_N - m_N^*)$  is well realized as is expected [14, 15].

Next, we consider potentials for the mesons in a nucleus. A detailed description of the Lagrangian density and the mean-field equations of motion needed to describe a finite nucleus is given in Refs. [12, 13]. At position  $\vec{r}$  in the nucleus (the coordinate origin is taken at the center of the nucleus), the Dirac equations for the quarks and antiquarks in

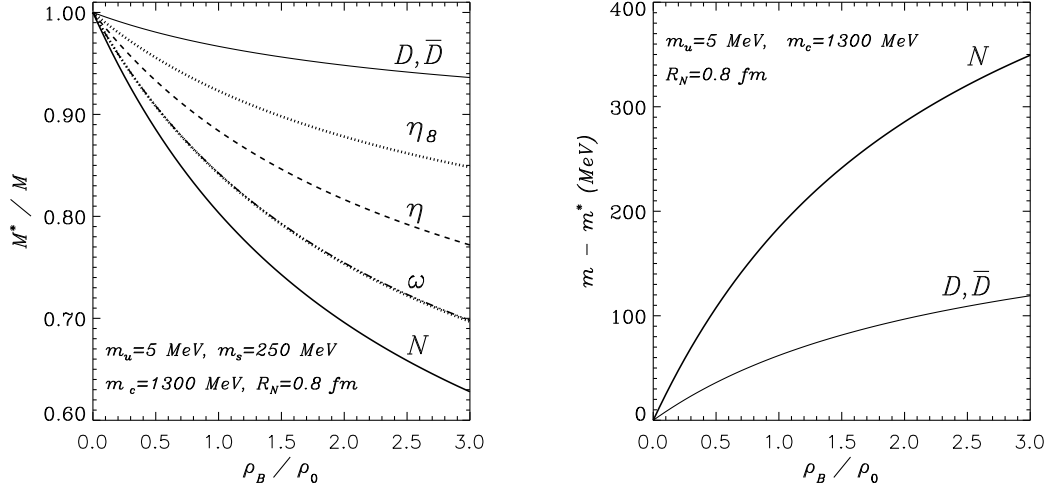


Figure 1: Effective masses of the nucleon, physical  $\eta$ , physical  $\omega$ ,  $D$  and  $\bar{D}$  mesons, and those calculated based on SU(3) quark model basis (the dotted lines), which are given in Eqs. (1) - (3). The two cases for the  $\omega$  meson are almost degenerate. (Normal nuclear matter density,  $\rho_0$ , is  $0.15 \text{ fm}^{-3}$ .)

the meson bags ( $|\vec{x} - \vec{r}| \leq \text{bag radius}$ ) are given by [10, 17, 19]:

$$\left[ i\gamma \cdot \partial_x - (m_q - V_\sigma^q(\vec{r})) \mp \gamma^0 \left( V_\omega^q(\vec{r}) + \frac{1}{2} V_\rho^q(\vec{r}) \right) \right] \begin{pmatrix} \psi_u(x) \\ \psi_{\bar{u}}(x) \end{pmatrix} = 0, \quad (4)$$

$$\left[ i\gamma \cdot \partial_x - (m_q - V_\sigma^q(\vec{r})) \mp \gamma^0 \left( V_\omega^q(\vec{r}) - \frac{1}{2} V_\rho^q(\vec{r}) \right) \right] \begin{pmatrix} \psi_d(x) \\ \psi_{\bar{d}}(x) \end{pmatrix} = 0, \quad (5)$$

$$[i\gamma \cdot \partial_x - m_{s,c}] \psi_{s,c}(x) \text{ (or } \psi_{\bar{s},\bar{c}}(x)) = 0. \quad (6)$$

The mean-field potentials for a bag centered at position  $\vec{r}$  in the nucleus, which are approximated to be constants in the entire bag volume, are defined by  $V_\sigma^q(\vec{r}) = g_\sigma^q \sigma(\vec{r})$ ,  $V_\omega^q(\vec{r}) = g_\omega^q \omega(\vec{r})$  and  $V_\rho^q(\vec{r}) = g_\rho^q b(\vec{r})$ , with  $g_\sigma^q$ ,  $g_\omega^q$  and  $g_\rho^q$  the corresponding quark and meson-field coupling constants. The mean meson fields, which will depend only on the distance,  $r = |\vec{r}|$ , are calculated self-consistently by solving Eqs. (23) - (30) of Ref. [13].

The corresponding quark eigenenergies in the bag in units of  $1/R_j^*$  ( $j = \eta, \omega, D, \bar{D}$ ) are given by [10, 17, 19]

$$\begin{pmatrix} \epsilon_u(\vec{r}) \\ \epsilon_{\bar{u}}(\vec{r}) \end{pmatrix} = \Omega_q^*(\vec{r}) \pm R_j^* \left( V_\omega^q(\vec{r}) + \frac{1}{2} V_\rho^q(\vec{r}) \right), \quad (7)$$

$$\begin{pmatrix} \epsilon_d(\vec{r}) \\ \epsilon_{\bar{d}}(\vec{r}) \end{pmatrix} = \Omega_q^*(\vec{r}) \pm R_j^* \left( V_\omega^q(\vec{r}) - \frac{1}{2} V_\rho^q(\vec{r}) \right), \quad (8)$$

$$\epsilon_{s,c}(\vec{r}) = \epsilon_{\bar{s},\bar{c}}(\vec{r}) = \Omega_{s,c}(\vec{r}), \quad (9)$$

where  $\Omega_q^*(\vec{r}) = \sqrt{x_q^2 + (R_j^* m_q^*)^2}$ , with  $m_q^* = m_q - g_\sigma^q \sigma(\vec{r})$  and  $\Omega_{s,c}(\vec{r}) = \sqrt{x_{s,c}^2 + (R_j^* m_{s,c})^2}$ . The bag eigenfrequencies,  $x_q$  and  $x_{s,c}$ , are determined by the usual, linear boundary condition [12, 13]. The meson masses in the nucleus at position  $\vec{r}$ , are calculated by (see

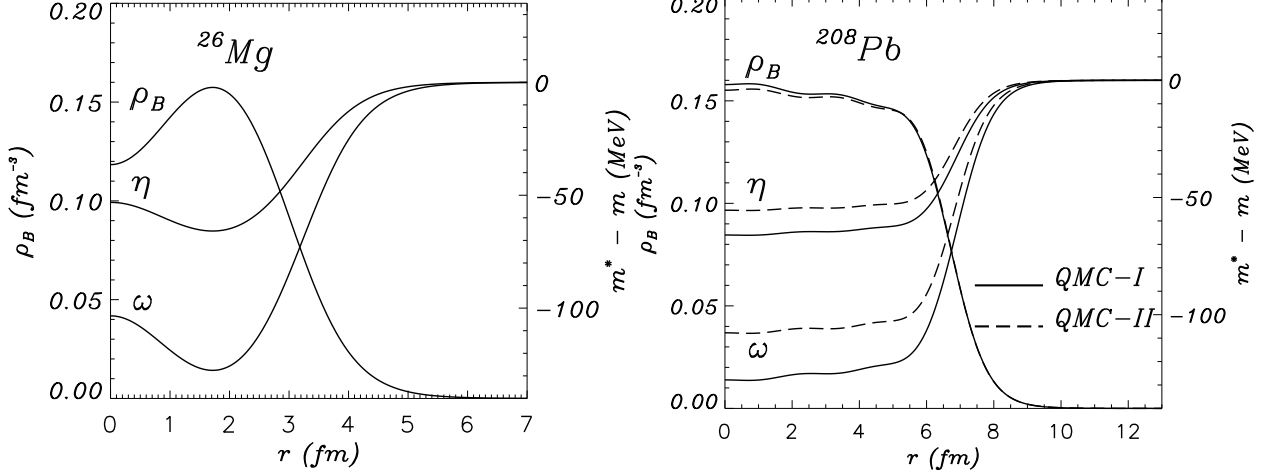


Figure 2: Potentials for the  $\eta$  and  $\omega$  mesons,  $(m_\eta^*(r) - m_\eta)$  and  $(m_\omega^*(r) - m_\omega)$ , calculated in QMC-I [13] for  $^{26}\text{Mg}$  and  $^{208}\text{Pb}$ . For  $^{208}\text{Pb}$  the potentials are also shown for QMC-II [14].

also Eqs. (1) - (3) for the  $\eta$  and  $\omega$ ):

$$m_{\eta,\omega}^*(\vec{r}) = \frac{2[a_{P,V}^2 \Omega_q^*(\vec{r}) + b_{P,V}^2 \Omega_s(\vec{r})] - z_{\eta,\omega}}{R_{\eta,\omega}^*} + \frac{4}{3} \pi R_{\eta,\omega}^3 B, \quad (10)$$

$$m_{D,\bar{D}}^*(\vec{r}) = \frac{\Omega_q^*(\vec{r}) + \Omega_c(\vec{r}) - z_{D,\bar{D}}}{R_{D,\bar{D}}^*} + \frac{4}{3} \pi R_{D,\bar{D}}^3 B, \quad (11)$$

$$\left. \frac{\partial m_j^*(\vec{r})}{\partial R_j} \right|_{R_j=R_j^*} = 0, \quad (j = \eta, \omega, D, \bar{D}), \quad (12)$$

with

$$a_{P,V} = \frac{1}{\sqrt{3}} \cos \theta_{P,V} - \sqrt{\frac{2}{3}} \sin \theta_{P,V}, \quad b_{P,V} = \sqrt{\frac{2}{3}} \cos \theta_{P,V} + \frac{1}{\sqrt{3}} \sin \theta_{P,V}. \quad (13)$$

In Eqs. (10), the constants  $z_j$  ( $j = \eta, \omega, D, \bar{D}$ ) parameterize the sum of the center-of-mass and gluon fluctuation effects, which are determined to reproduce the corresponding physical meson masses in free space. Note that  $z_j$  and  $B$  are independent of density.

In this study we chose the values,  $(m_q, m_s, m_c) = (5, 250, 1300)$  MeV for the current quark masses, and  $R_N = 0.8$  fm for the bag radius of the nucleon in free space. (The other input parameters at the quark and hadronic levels are given in Refs. [10, 13, 17].) We stress here that exactly the same coupling constants in QMC,  $g_\sigma^q$ ,  $g_\omega^q$  and  $g_\rho^q$ , are used for the light quarks in the mesons as in the nucleon. However, in studies of the kaon system, we found that it was phenomenologically necessary to increase the strength of the vector coupling to the non-strange quarks in the  $K^+$  ( $g_\omega^q \rightarrow 1.4^2 g_\omega^q$ ) in order to reproduce the empirically extracted  $K^+$ -nucleus interaction [19]. It is not yet clear whether this is a specific property of the  $K^+$ , which is a pseudo-Goldstone boson, or a general feature of the interaction of a light quark. Thus, we show results for the  $\bar{D}$  bound state energies with both choices for this potential, in order to test the theoretical uncertainty. For the larger  $\omega$  meson coupling, suggested by  $K^+A$  scattering,  $V_\omega^q(r)$  is replaced by  $\tilde{V}_\omega^q(r) = 1.4^2 V_\omega^q(r)$ .

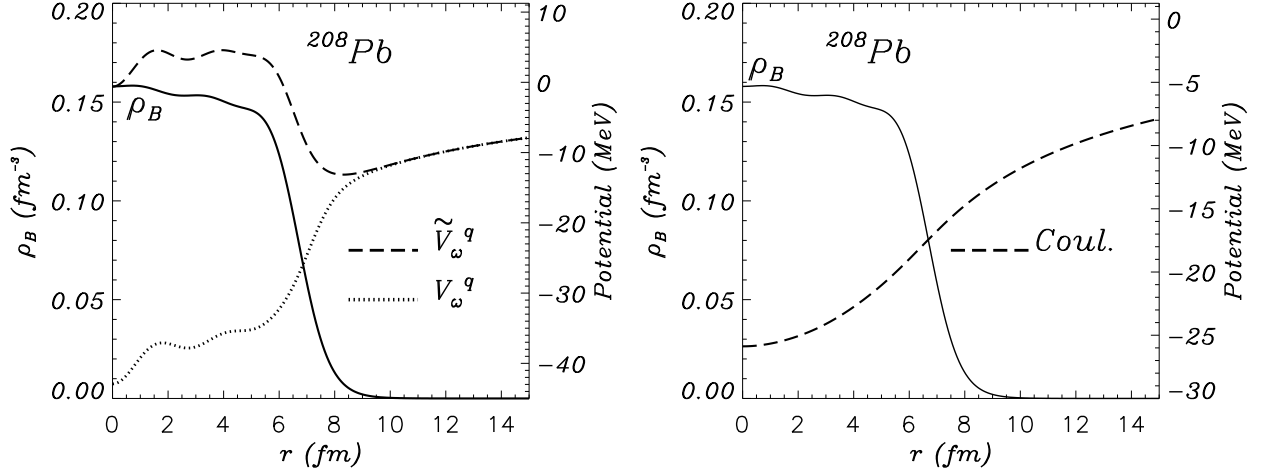


Figure 3: The left panel shows sum of the scalar, vector and Coulomb potentials for the  $D^-$  meson in  $^{208}\text{Pb}$  for two cases,  $(m_{D^-}^*(r) - m_{D^-}) + \tilde{V}_\omega^q(r) + \frac{1}{2}V_\rho^q(r) - A(r)$  (the dashed line) and  $(m_{D^-}^*(r) - m_{D^-}) + V_\omega^q(r) + \frac{1}{2}V_\rho^q(r) - A(r)$  (the dotted line), where  $\tilde{V}_\omega^q(r) = 1.4^2 V_\omega^q(r)$ . The right panel shows the Coulomb potential.

Note that the  $\rho$  meson mean field potential,  $V_\rho^q(r)$ , is negative in a nucleus with a neutron excess, such as e.g.,  $^{208}\text{Pb}$ .

In Figs. 2 and 3 we show the calculated potentials, for the  $\eta$  and  $\omega$ , and the  $D^-$  mesons, respectively. For the  $D^-$  we show also the Coulomb potential which ensures the formation of atomic bound states. The left panel in Fig. 3 shows the *naive* sum of the scalar and vector potentials for the  $D^-$ , for the two choices of the vector potentials,  $\tilde{V}_\omega^q(r)$  (the dashed line) and  $V_\omega^q(r)$  (the dotted line), while the right panel shows the Coulomb potential.

Because the  $D^-$  meson is heavy and may be described well in the (nonrelativistic) Schrödinger equation, one expects the existence of the  $^{208}\text{Pb}$  bound states just from inspection of the *naive* sum of the potentials, in a way which does not distinguish the Lorentz vector or scalar character.

### 3 Results

Here we calculate the bound state energies for the mesons using the mean field potentials obtained in QMC. We consider the situation of almost zero momentum for the mesons. Then, after imposing the Lorentz condition, solving the Proca equation becomes equivalent to solving the Klein-Gordon equation, because the transverse and longitudinal masses for the vector meson are degenerate. Thus, we may solve the following form of the Klein-Gordon equation for the  $\eta$ ,  $\omega$ ,  $D$  and  $\bar{D}$  mesons:

$$[\nabla^2 + (E_j - V_v^j(r))^2 - \tilde{m}_j^{*2}(r)] \phi_j(\vec{r}) = 0, \quad (j = \eta, \omega, D, \bar{D}), \quad (14)$$

with

$$\tilde{m}_j^*(r) = m_j^*(r) - \frac{i}{2} [(m_j - m_j^*(r))\gamma_j + \Gamma_j] \equiv m_j^*(r) - \frac{i}{2}\Gamma_j^*(r), \quad (15)$$

Table 1: Calculated  $\eta$  and  $\omega$  meson bound state energies (in MeV),  $E_j = Re(E_j^*)$  ( $j = \eta, \omega$ ), in QMC [10] and those of the  $\omega$  in the Walecka model with  $\sigma$ - $\omega$  mixing effect [22]. The complex eigenenergies are given by,  $E_j^* = E_j + m_j - i\Gamma_j/2$ .

		$\gamma_\eta = 0.5$ (QMC)	$\gamma_\omega = 0.2$ (QMC)	$\gamma_\omega = 0.2$ (QHD)			
		$E_\eta$	$\Gamma_\eta$	$E_\omega$	$\Gamma_\omega$	$E_\omega$	$\Gamma_\omega$
${}^6_j\text{He}$	1s	-10.7	14.5	-55.6	24.7	-97.4	33.5
${}^{11}_j\text{B}$	1s	-24.5	22.8	-80.8	28.8	-129	38.5
${}^{26}_j\text{Mg}$	1s	-38.8	28.5	-99.7	31.1	-144	39.8
	1p	-17.8	23.1	-78.5	29.4	-121	37.8
	2s	—	—	-42.8	24.8	-80.7	33.2
${}^{16}_j\text{O}$	1s	-32.6	26.7	-93.4	30.6	-134	38.7
	1p	-7.72	18.3	-64.7	27.8	-103	35.5
${}^{40}_j\text{Ca}$	1s	-46.0	31.7	-111	33.1	-148	40.1
	1p	-26.8	26.8	-90.8	31.0	-129	38.3
	2s	-4.61	17.7	-65.5	28.9	-99.8	35.6
${}^{90}_j\text{Zr}$	1s	-52.9	33.2	-117	33.4	-154	40.6
	1p	-40.0	30.5	-105	32.3	-143	39.8
	2s	-21.7	26.1	-86.4	30.7	-123	38.0
${}^{208}_j\text{Pb}$	1s	-56.3	33.2	-118	33.1	-157	40.8
	1p	-48.3	31.8	-111	32.5	-151	40.5
	2s	-35.9	29.6	-100	31.7	-139	39.5

where  $E_j$  is the total energy of the meson (the binding energy is  $E_j - m_j$ ),  $V_v^j(r)$ ,  $m_j$  and  $\Gamma_j$  are the sum of the vector and Coulomb potentials, the corresponding masses and widths in free space [18, 10, 17], and  $\gamma_j$  are treated as phenomenological parameters to describe the in-medium meson widths,  $\Gamma_j^*(r)$ . According to the estimates in Refs. [7, 21], the widths of the mesons in nuclei and at normal nuclear matter density are,  $\Gamma_\eta^* \sim 30 - 70$  MeV [7] and  $\Gamma_\omega^* \sim 30 - 40$  MeV [21], respectively. Thus, we show the bound state energies calculated for the values of the parameters,  $\gamma_\eta = 0.5$  and  $\gamma_\omega = 0.2$ , which are expected to correspond best with experiment. For the  $D^-$  and  $\bar{D}^0$ , the widths are set to zero which is exact, whereas those for the  $D^0$  does not make sense. Nevertheless, some results for the  $D^0$  calculated using the zero width will be listed for the purpose of comparison. Eq. (14) is solved in momentum space [20], where extra care is taken for the treatment of the long range Coulomb potential for the  $D^-$  (see Refs. [17, 20]).

The calculated meson-nucleus bound state energies are listed in Tables 1 and 2. Results for the  $\omega$ -meson are also shown for the Walecka model [22].

## 4 Summary

We have investigated several possible meson-nucleus bound states using QMC. Our results suggest that  $\eta$  and  $\omega$  mesons should be bound in all the nuclei considered. Furthermore, the  $D^-$  meson should inevitably be bound in  ${}^{208}\text{Pb}$ , due to two quite different mechanisms,

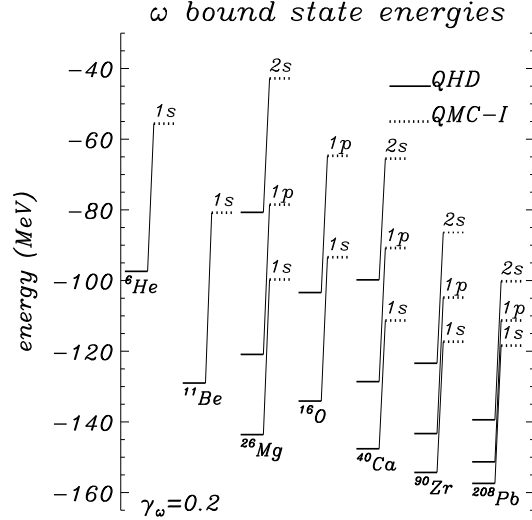


Figure 4: Calculated  $\omega$  meson bound state energy levels in QHD and QMC. Detailed data for QMC can be seen in Ref.[10].

Table 2: Calculated  $D^-$ ,  $\bar{D}^0$  and  $D^0$  meson bound state energies (in MeV) in  $^{208}\text{Pb}$  for different potentials. The widths for the mesons are all set to zero, both in free space and inside  $^{208}\text{Pb}$ . Note that the  $D^0$  bound states energies calculated with  $\tilde{V}_\omega^q$  will be much larger than those calculated with  $V_\omega^q$  (in absolute value).

state	$D^-(\tilde{V}_\omega^q)$	$D^-(V_\omega^q)$	$D^-(V_\omega^q, \text{no Coulomb})$	$\bar{D}^0(\tilde{V}_\omega^q)$	$\bar{D}^0(V_\omega^q)$	$D^0(V_\omega^q)$
1s	-10.6	-35.2	-11.2	unbound	-25.4	-96.2
1p	-10.2	-32.1	-10.0	unbound	-23.1	-93.0
2s	-7.7	-30.0	-6.6	unbound	-19.7	-88.5

namely, the scalar and attractive  $\sigma$  mean field, with the assistance of the Coulomb force. The existence of any bound states at all would give us important information concerning the role of the Lorentz scalar  $\sigma$  field, and hence dynamical symmetry breaking; in other words, information on the partial restoration of chiral symmetry in medium.

### Acknowledgement

The author would like to thank D.H. Lu, K. Saito and A.W. Thomas for exciting collaborations. The results reported here are based on the work investigated together with them. This work was supported by the Australian Research Council.

## References

- [1] Quark Matter '97, to be published in Nucl. Phys. **A** (1998).
- [2] P. Wurm for the CERES collaboration, Nucl. Phys. **A590**, 103c (1995).

- [3] M. Masera for the HELIOS collaboration, Nucl. Phys. **A590**, 93c (1995).
- [4] G.Q. Li, C.M. Ko and G.E. Brown, Nucl. Phys. **A606**, 568 (1996); G. Chanfray, R. Rapp and J. Wambach, Phys. Rev. Lett. **76**, 368 (1996).
- [5] M. Kossov *et al.*, TJNAF proposal PR-94-002 (1994); P.Y. Bertin and P.A.M. Guichon, Phys. Rev. C **42**, 1133 (1990).
- [6] HADES proposal, HADES home page: <http://piggy.physik.uni-giessen.de/hades/>; G.J. Lolos *et al.* Phys. Rev. Lett. **80**, 241 (1998).
- [7] R.S. Hayano *et al.*, proposal for GSI/SIS, September, 1997; R.S. Hayano, 2nd Int. Symp. on Symmetries in Subatomic Physics, Seattle (1997).
- [8] R.S. Hayano, S. Hirenzaki and A. Gillitzer, nucl-th/9806012.
- [9] F. Klingl, T. Waas and W. Weise, hep-ph/9810312.
- [10] K. Tsushima, D.H. Lu, A.W. Thomas, K. Saito, nucl-th/9806043, to appear in Phys. Lett. B.
- [11] P.A.M. Guichon, Phys. Lett. B **200**, 235 (1988).
- [12] P.A.M. Guichon, K. Saito, E. Rodionov and A.W. Thomas, Nucl. Phys. **A601**, 349 (1996).
- [13] K. Saito, K. Tsushima and A.W. Thomas, Nucl. Phys. **A609**, 339 (1996).
- [14] K. Saito, K. Tsushima and A.W. Thomas, Phys. Rev. C **55**, 2637 (1997).
- [15] K. Tsushima, K. Saito, J. Haidenbauer, A.W. Thomas, Nucl. Phys. **A630**, 691 (1998).
- [16] For recent results of QMC, A.W. Thomas, nucl-th/9807027.
- [17] K. Tsushima, D.H. Lu, A.W. Thomas, K. Saito and R.H. Landau, ADP-98-48/T317, OSUNT98-13, nucl-th/9810016, submitted to Phys. Rev. C (1998).
- [18] Review of Particle Physics, Phys. Rev. D **54**, 1 (1996).
- [19] K. Tsushima, K. Saito, A.W. Thomas and S.W. Wright, Phys. Lett. B **429**, 239 (1998); *ibid* (E) to appear in Phys. Lett. B (typos,  $g_{K\omega}^q = g_{\omega}^K = 1.4 \times g_{\omega}^q$ , should be replaced by  $g_{K\omega}^q = g_{\omega}^K = 1.4^2 \times g_{\omega}^q$ ).
- [20] R.H. Landau, *Quantum Mechanics II* (John Wiley & Sons, New York, 1990); Y.R. Kwon and F. Tabakin, Phys. Rev. C **18**, 932 (1978); D.H. Lu and R.H. Landau, Phys. Rev. C **49**, 878 (1994).
- [21] B. Friman, nucl-th/9801053; F. Klingl and W. Weise, hep-ph/9802211.
- [22] K. Saito, K. Tsushima, D.H. Lu and A.W. Thomas, nucl-th/9807028, to appear in Phys. Rev. C.